World Academy of Science, Engineering and Technology
International Journal of Chemical and Materials Engineering
Vol:15, No:11, 2021

Combination of Tensile Strength and Elongation of Reverse Rolled TaNbHfZrTi Refractory High Entropy Alloy

M. Veerasham

***Abstract*—**The refractory high entropy alloys are potential materials for high-temperature applications because of their ability to retain high strength up to 1600°C. However, their practical applications were limited due to poor elongation at room temperature. Therefore, decreasing the average valence electron concentrations (VEC) is an effective design strategy to improve the intrinsic ductility of refractory high entropy alloys. In this work, the high-entropy alloy TaNbHfZrTi was processed at room temperature by each step reverse rolling up to a 90% reduction in thickness. Subsequently, the reverse rolled 90% samples were utilized for annealing treatment at 800°C and 1000°C for 1 h to understand phase stability, microstructure, texture, and mechanical properties. The reverse rolled 90% condition contains body-centered cubic (BCC) single-phase; upon annealing at 800 °C, the formation of secondary phase BCC-2 prevailed. The partial recrystallization and complete recrystallization microstructures were developed for annealed at 800°C and 1000°C, respectively. The reverse rolled condition and 1000°C annealed temperature exhibit extraordinary room temperature tensile properties with high ultimate tensile strength (UTS) without compromising loss of ductility called "strength-ductility" trade-off. The reverse-rolled 90% and annealing treatment carried out at temperature about 1000°C for 1 h consist of UTS 1430 MPa and 1556 MPa with an appreciable amount of 21% and 20% elongation, respectively. The development of hierarchical microstructure prevailed for the annealed 1000°C which led to the simultaneous increase in tensile strength and elongation.

***Keywords*—**Refractory high entropy alloys, reverse rolling, recrystallization, microstructure, tensile properties.

I. Introduction

THE metallic materials are the backbone for manufacturing industries because of their outstanding load-bearing capacity, elongation, and damage tolerance. The high entropy alloys (HEAs) are new generation metallic materials possessing higher configurational entropy, which stabilizes simple solid solutions like BCC, face-centered cubic (FCC), and BCC+FCC [1]-[3]. The sluggish diffusion property of HEAs slows down the kinetics of diffusion, and it helps develop materials for high-temperature applications [4]. The refractory high entropy alloys (RHEAs) are a new generation of potential high-temperature materials based on the refractory elements such as TaCrMoTiZrHfVNbW. The RHEAs were first introduced in 2010 and then instantly attracted attention due to their immense ability to retain high strength up to 1600 °C. The first developed RHEAs were based on five refractory elements (V, Mo, W, Ta, and Nb), but later the choice of the alloying elements was expanded to include other alloying elements, such as Group IV (Zr, Hf, and Ti), Group V (Nb, V, and Ta), and Group VI (W, Cr, and Mo) elements. In addition, the RHEAs may contain minor alloying addition, e.g., Al, to improve their properties [5]-[10].

It is known that generally, softening occurs at temperatures above 0.6 Tm of the absolute melting point of an alloy. Then the increasing alloy melting temperature through suitable alloying may increase operating temperature, and thus such high melting points of refractory metals and alloys make them useful for application at elevated temperatures beyond Ni, Co, and steel-based superalloys. The majority of the RHEAs have a BCC crystal structure and may also contain inter-metallic (IM) phases, such as B2, Laves phases [7]. The RHEAs have greater specific strengths at temperatures of 1000-1600 °C. Nevertheless, the biggest challenge is extremely poor room temperature (RT) ductility, high density, and poor oxidation resistance properties limit the applications [6]-[9]. These challenges need to be overcome for the accelerated industrial applications of the RHEAs. In particular, processing the RHEAs at RT remains a challenge owing to their poor ductility. On the other hand, processing at elevated temperatures is often cost-intensive. Therefore, there is an urgent need to develop RHEAs, which can be successfully processed at ambient temperatures. There are two possible approaches to improve ductility design. One is the usual approach based on the microstructural design approach of modifying grain size, precipitate distribution, etc. called 'extrinsic ductility'. The other way is based on improving ductility in the BCC perfect crystal structure called 'intrinsic ductility'. The intrinsic ductility changes failure mode from brittle failure to ductile failure. In the perfect crystalline structures even though the applied loading direction is perpendicular to the cleavage plane, the dislocation nucleation will be activated before crack formation so that they fail by ductile manner [10].

The RHEAs containing elements from groups VI, V, and IV tend to form single-phase bcc solid solutions. From the theoretical analysis and available experimental results, decreasing the average valence electron numbers, or valence electron concentrations, VEC = $\sum_{i=1}^{n} C_i (VEC)i$, [1], [2] has been proved to be effective in designing RHEAs. Interestingly, all ductile RHEAs have a VEC less than 4.4, and RHEAs with a VEC greater than 4.6 would be brittle, whereas RHEAs with a VEC of 4.5 would be ductile or brittle. Further various authors

M. Veerasham is with Department of Materials Science and Metallurgical Engineering, IIT Hyderabad, India (e-mail: ms15resch11003@iith.ac.in).

considered theoretical analysis of these aspects [1], [2], [7].

Thermo-mechanical processing (TMP) of materials combining heavy deformation and thermal treatments can significantly enhance engineering materials' properties. An area of prime interest in the HEA research is designing appropriate TMP routes for developing HEAs with improved properties through microstructure and texture control. Therefore, understanding the microstructure and texture evolution during TMP remains critical.

While TMP treatments in other HEAs are already being investigated, the possibilities of TMP treatments of refractory HEAs, particularly at ambient temperatures, have remained mostly unexplored. Demand and pursuit of metallic materials with higher strength, ductility and thermal stability have never faded for practical applications. The cross-section area (A) of the specimen can be reduced as the enhancement of materials tensile strength (σ) for sustaining a particular load (P). From the well-known definition of stress: $\sigma = P/A$ it provides the required inputs for using high tensile strength for manufacturing thin engineering materials; it leads to substantial weight and more significant environmental savings. Nevertheless, unfortunately, the tensile strength increment is typically accompanied by the sacrifice of elongation called the "strength-ductility" trade-off; the controlled microstructure features development substantially helps to improve tensile strength without loss ductility [11]. In the present research, we explored to achieve remarkable refractory-HEA alloy which shows appreciable ductility and after that surpass "strength-ductility" trade-off, through TMP treatments by each step reverse-rolling and annealing, and associated developments in microstructure, texture, and properties.

II. Experimental Procedure

A. Processing

The RHEA alloy was cast by melting several times in an arc melting furnace, starting with individual TaNbHfZrTi elements. The as-cast of this alloy is polished mechanically and subsequently cold-rolled 50% in several passes and annealed at 1400 °C for 10 min; after that, this sample is used as starting material for further deformation process. The starting material each step reverse rolled 90% (rolling direction changed to 180° degrees in each step) in multiple passes at RT. The reverse-rolled specimens are subjected to an annealing treatment at 800 °C and 1000 °C for 1 h followed by quenching in water, and these reverse-rolled and annealed specimens are taken for characterization. The reverse-rolled samples were encapsulated in a quartz tube under vacuum to hinder oxidation during heat treatment.

B. Characterization

The phase analysis of the RHEA was carried out using X-ray diffraction (PANalytical, The Netherlands; Model: X'Pert PRO). The microstructure and texture exploration of the reverse rolled and annealed specimens were experimented by utilizing the electron backscatter diffraction (EBSD) technique (Oxford Instruments, UK; has an attachment to SEM (scanning electron microscope, Carl-Zeiss, Germany; Model: SUPRA 40)). The specimens for EBSD investigations were prepared through the electropolishing method (electrolyte: perchloric acid and methanol with 1:9 ratios by volume). The EBSD scans were obtained through the AztecHKL software. The obtained EBSD dataset was transmitted to the TSL-OIM™ software (EDAX Inc., USA). The tensile test (UTM) for all the specimens was carried out at 10^{-3} mm/sec strain rate by using a universal testing machine (UTM) model (Instron 5967, embedded with digital image capture (DIC)) at room temperature (RT).

III. Results

A. Reverse Rolled Microstructure and Texture of TaNbHfZrTi Alloy

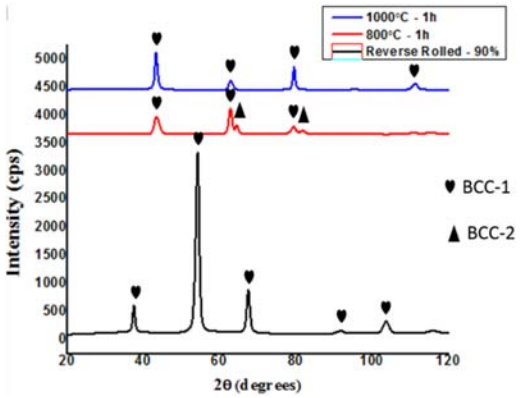

Fig. 1 XRD graph of TaNbHfZrTi reverse-rolled and annealed at 800 °C and 1000 °C for 1 h

The X-ray diffraction (XRD) pattern of the reverse rolled 90% alloy Fig. 1 peaks of only single-phase BCC are observed. Figs. 2 (a) and (b) reveal the TaNbHfZrTi microstructure after 90% novel reverse rolling. Curiously, the reverse rolled 90% alloy exhibits microstructure inhomogeneity presence of non-lamellar and fine lamellar regions (regions marked by a yellow ellipse and a red arrow respectively) consists of very fine grain size of ~0.80 μm (Table I) and their distribution is shown in Fig. 4. The heterogeneous microstructure shows severely deformed regions (shown with a green ellipse) and regions with elongated grains along the rolling direction (RD) (highlighted with white arrow) and also extensive development of shear and deformation bands is noticed. The fragmentation of shear bands would be another mechanism to find grains development and refinement of microstructure, quite distinct phenomena for higher strains. These shear bands are oriented parallel (~ 35^0 degrees) to RD. Moreover, fine grains are situated at grain boundaries of the primarily bent grains in Figs. 2 (a) and (b).

Fig. 3 (a) is the $\varphi_2 = 45°$ section of ODFs of reverse-rolled 90% TaNbHfZrTi alloy. The texture development from the ODF section shows the presence of RD and ND fiber texture. The {001} <1-10>, {113} <1-10> and {113} <1-10> showed maximum intensity, which is an essential component of RD fiber, and the maximum intensity is present at {111} <112> on the ND fiber texture and other small intensity contours can be seen present at various locations.

B. Annealed Microstructure and Texture of TaNbHfZrTi

Alloy

Fig. 1 is the XRD graph of annealed specimens at different temperatures 800 °C and 1000 °C for 1 h. The graph reveals that both annealed temperatures containing the BCC – 1 phase and annealed at 800 °C for 1 h show the evolution of the second phase BCC – 2 because very fine particle size identification was not possible in SEM imaging. This second phase BCC-2 decomposed back into the matrix for 1000 °C annealed temperature. Figs. 2 (c) and (d) reveal the EBSD maps of the annealed TaNbHfZrTi RHEA.

TABLE I
THE AVERAGE GRAIN SIZE OF REVERSE-ROLLED AND ANNEALED TEMPERATURES

	Reverse Rolled-90%	800 °C	1000 °C
Average Grainsize (μm)	0.80	1.78	16.32

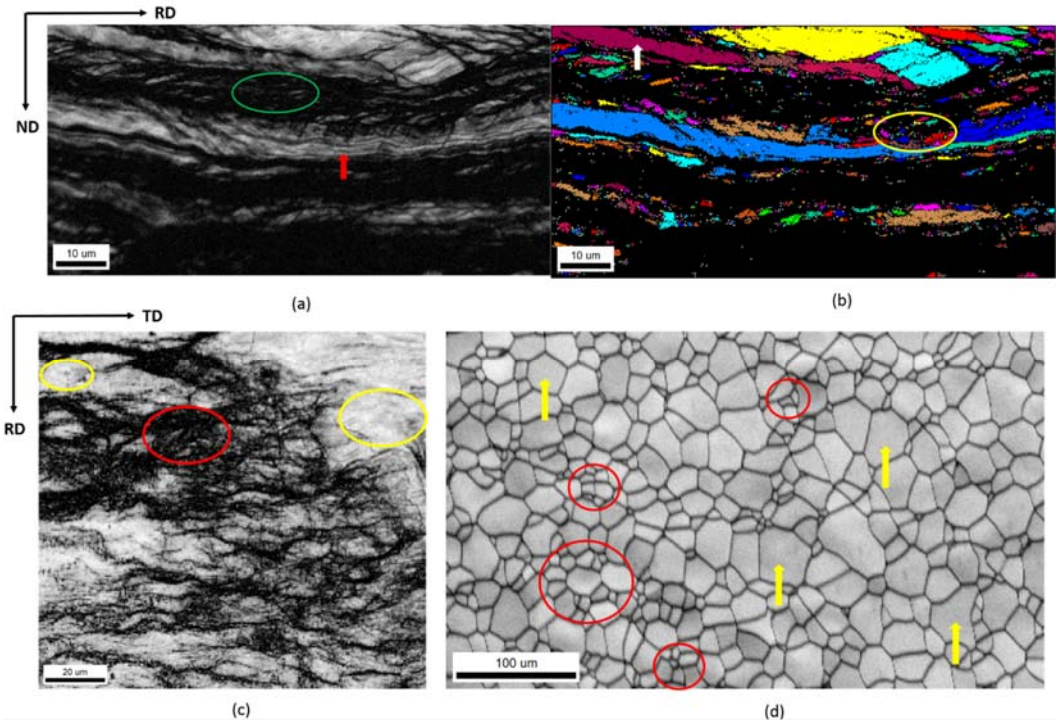

Fig. 2 (a) and (b) EBSD unique grain color map of reverse rolled condition and (c) and (d) annealed at 800°C and 1000°C temperatures for 1 h

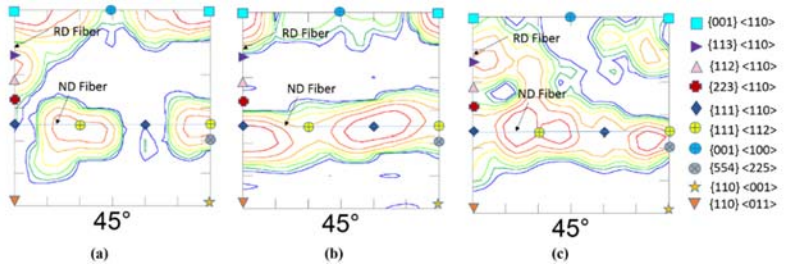

Fig. 3 φ2 = 45° sections of ODFs of TaNbHfZrTi reverse-rolled and annealed at 800 °C and 1000 °C for 1 h

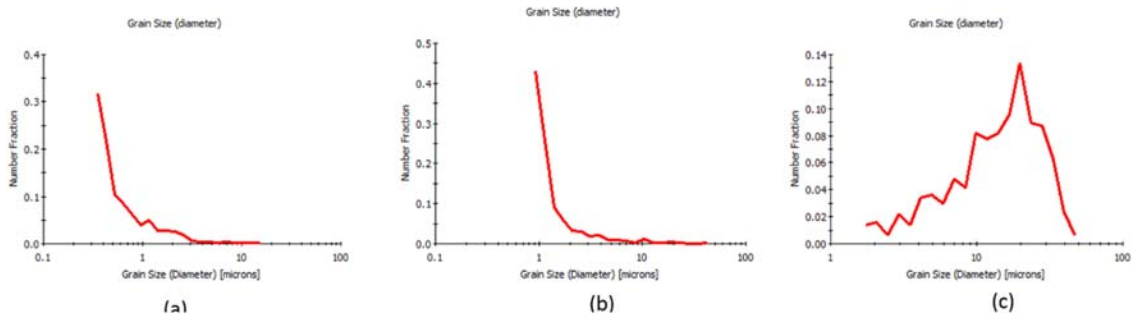

Fig. 4 The grain-size distribution of reverse-rolled and annealed at (a) 800 °C and (b)1000 °C for 1 h

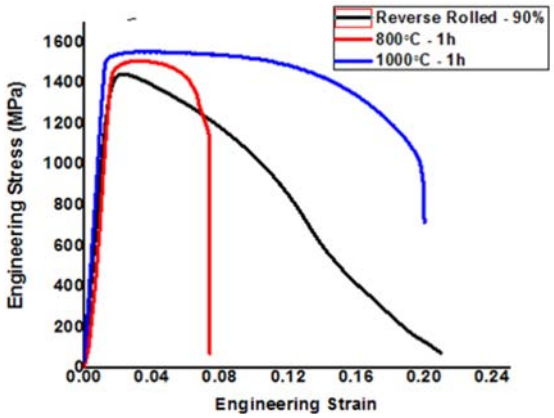

Fig. 5 Tensile graph of reverse rolled 90% and annealed at 800 °C and 1000 °C for 1 h

The annealed TaNbHfZrTi alloy at 800 °C for 1 h consists of very fine grains of ~1.78 μm in size (Fig. 2 (c)) (Table I) and their distribution is shown in Fig. 4. In the annealed microstructure, fine recrystallized grains are mixed with non-recrystallized grains. Further annealed microstructure at 1000 °C for 1 h has an average grain size of ~16.32 μm (Table I), and their distribution is shown in Fig. 4. The development of coarse microstructure featured for annealing treatment at 1000 °C temperature in comparison to rolled condition and annealed at 800 °C temperature. Most of the recrystallized grains are linearly inclined along with the 35–65^0 degrees to the RD because the recrystallization starts preferentially along the 35–65^0 degrees' shear bands evolved in reverse rolling. The annealing process carried out at 1000 °C temperature resulted in hierarchical microstructure evolution consisting of a range of grain sizes distribution in the microstructure, which clearly reveals that unstable recrystallized bigger grains were consuming fine grains during grain growth. In other regions, equiaxed grains were observed most of them turning into faceted as the grain size is rising by consuming fine grains.

The texture development during the annealing process at 800 °C and 1000 °C temperatures are interpreted by constant φ2 = 45^o sections of ODFs, Figs. 3 (b) and (c). The evolution of ND and RD fiber texture has prevailed for 800 °C temperature annealed condition. The maximum ODF intensity showed at {001} <1-10> orientation of RD fiber and {111} <112> orientation of ND fiber texture components. Further annealing treatment carried out at 1000 °C revealed ND and RD fiber texture development.

C. Tensile Properties of TaNbHfZrTi Alloy

Fig. 5 is tensile test curves of reverse-rolled – 90% and annealed 800 °C and 1000 °C. The reverse rolled condition consists of incredible tensile strength and ductility is shows yield stress 1045 MPa after that continues strain hardening. The strain hardening occurred up to UTS of 1430 MPa within the engineering strain of 2.3 percentage (uniform elongation). After UTS, the elongation continued, and further, it is noticeable that a continuous load drop until engineering elongation reaches 21%. The fracture occurred at stress 75 Mpa and strained 21%. The continuous load drop is the witness of localized deformation and neck formation. Annealing at 800 °C for 1 h exhibits a similar strain hardening trend and rises maximum stress to UTS 1515 MPa after UTS non-uniform deformation continues up to fracture stress of 1151 MPa and strain of 7% the non-uniform deformation is approximately four times lesser than reverse rolled condition. Furthermore, the annealing process carried out at 1000 °C temperature for 1 h reveals uniform deformation until the UTS 1556 MPa. The UTS prevailing in the case of 1000 °C temperature heat treatment is higher than both reverse-rolled and 800 °C annealed conditions, then the non-uniform deformation continues until fracture stress of 996 MPa and 20% elongation. The rolled and annealed 1000 °C temperature exhibits outstanding tensile strength and ductility.

IV. Discussion

The microstructure evolution of profoundly reverse rolled condition was resulted by grain subdivision at various length scales. In the BCC structured materials, the formation of deformation bands and shear bands are typically noticed at high deformation. The various parts grain rotations to completely different thermodynamically stable orientations would result in the evolution of localized texture [12], [13]. The severely deformed strain can be accumulated by formation dislocations and by the development of new boundaries. Low angle grain boundaries (LAGBs) conversion happens into deformation-induced high angle grain boundaries (HAGBs) due to the accumulation of dislocations. The grains are subdivided, resulting in increasing finer grain size [12]-[14]. The grain refinement mechanisms by plastic deformation were not completely understood and needed to be explored in the future to understand precise mechanisms. The possible understandable mechanism is the development of a dislocation structure that gently transforms as new small grain structures by the accumulation of misorientation among the neighboring dislocation cells and subgrains intersection of micro-bands Thus, it leads to microstructure refinement and even nanoscale microstructure [12]-[14]. The stored energy in the highly deformed microstructure causes recrystallization when the highly strained deformed microstructure is subject to annealing above the recrystallization temperature. The increment of grain growth in the annealing process was attributed to non-equilibrium boundaries that provide significant boundary mobility [14]. During annealing, a heavily deformed alloy may experience the following changes in the microstructure: recovery of the dislocation structures, unstable grain boundary transforming to the equilibrium grain boundary, and grain structure becoming coarser and more equiaxed facet grains [14].

The deformation and heat-treatment processing of single-phase BCC structured metals and alloys texture are characterized by the formation of ND (ND//<111>) and RD (RD//<110>) fiber texture. The strength of the typical RDs-fiber components including {001} <110>, {113} <110>, {112} <110> and {223} <110> increases uniformly up to 70% rolling reduction, while the {112)} <110>, and {111} <110> components are strengthened thereafter. The ND-fiber does not

strengthen significantly up to a rolling reduction of 80%. However, with further deformation, at higher deformation, the ND-fiber components {111} <110> and {111} <112> preferentially strengthen [14], [15]. The formation of ND-fiber texture components after annealing treatment is favored by recrystallization because of higher stored energy in the deformed matrix, typical behavior of annealing texture evolution in BCC structured materials RD-fiber components usually show recovery behavior [15].

The microstructure of 800 °C annealed condition was consisting of non-recrystallized and recrystallized grains. The enhancement of tensile strength is quite common due to the effect of the non-recrystallized grains. The most outstanding feature of the hierarchical microstructure (fine grains and large grains) of the annealed 1000 °C RHEA is achieving the simultaneous increase in strength and ductility. The simultaneous rise in strength-ductility was demonstrated in the previous investigations [16]-[19] of HEAs due to TRIP and deformation twinning. According to the Hall-Patch equation, the yield stress (YS) is inversely proportional to grain size (D), which means yield strength increases with decreasing grain size. The hierarchical microstructure existing of hard and soft domains was clarified [10], [16]-[19]. The deformation in the non-homogeneous microstructures typically occurs in three separate stages. The 1st stage is only an elastic stage of deformation both hard (small grains region) and soft domains in the hierarchical microstructure deform elastically similar to the conventional homogeneous microstructure. Next is 2nd stage, plastic deformation occurs in one domain, the one hand the soft (large grains) domains will begin deforming plastically, on the other hand, the hard (fine grains) domains will hinder plastic deformation. Thereby, soft domains can deform plastically easily. It results in the development of plastic strain gradients in hierarchical microstructure at the domain interface.

The plastic strain gradients commonly have to be accommodated by geometrically necessary dislocations (GNDs), significantly influencing the strength and leading to an adequate strengthening of the soft grains. Whenever in the hierarchical microstructure, large grains are surrounded by fine grains, GNDs will stock up at the boundaries of the domain, which results in high back stress. Entirely it will result in substantially high tensile yield strength than that expected employing the simple rule of mixtures. In the 3rd stage, both hard and soft domains (small and large grains regions respectively) will begin plastic deformation. However, the soft domains will experience enormous strain than hard domains [16]-[19]. Whenever the closest two different domains are subjected to different strain levels, the strain gradients would build up near the boundaries of the domain. The strain gradient rises with an increment of strain partitioning, providing substantial back stress work hardening. The presence of strain gradients in hierarchical microstructure with variation in hardness domains would be associated with more considerable back stress strengthening. The investigation on RHEA TaNbHfZrTi demonstrates the potential of reverse-rolling and annealing at 1000 °C temperature with an impressive balance between tensile strength and elongation.

IV. Conclusion

In the present investigation, the refractory-HEA TaNbHfZrTi alloy was prepared through an arc melting furnace. To explore the evolution of deformation and annealing microstructure, texture, and mechanical properties, the TaNbHfZrTi alloy was subjected to severe deformation through reverse rolling up to a 90% reduction in thickness and followed by annealing treatment at 800 °C and 1000 °C temperatures. The microstructure, after 90% reverse rolling, revealed substantial heterogeneity. XRD results showed that upon annealing at 800 °C temperature the formation of secondary phase BCC-2 prevailed. The hierarchical microstructure (fine grains and large grains) featured for the annealed 1000 °C condition lead to the simultaneous increase in strength and ductility. The reverse rolled condition, and 1000 °C annealed temperature consists of excellent RT tensile properties with appreciable tensile strength and a substantial elongation. The RD and ND fiber textures developed for the deformation and annealed conditions usual behavior for BCC structure materials.

Acknowledgments

The author acknowledges Dr. P.P. Bhattacharjee, MHRD, for providing fellowship, DST for funding equipment at the IIT Hyderabad, India. The author acknowledges Dr. Jien-Wei Yeh, National Tsing Hua University, Taiwan, for kindly providing the as-cast TaNbHfZrTi.

References

[1] Miracle, D. B., & Senkov, O. N. (2017). A critical review of high entropy alloys and related concepts. Acta Materialia, 122, 448-511.
[2] Murty, B. S., Yeh, J. W., Ranganathan, S., & Bhattacharjee, P. P. (2019). High-entropy alloys. Elsevier.
[3] Veeresham, M. Development of Impressive Tensile Properties of Hybrid Rolled Ta0.5Nb0.5Hf0.5ZrTi1.5 Refractory High Entropy Alloy. International Journal of Mechanical and Materials Engineering 15.6 (2021): 267-271.
[4] Tsai, K. Y., Tsai, M. H., & Yeh, J. W. (2013). Sluggish diffusion in Co–Cr–Fe–Mn–Ni high-entropy alloys. Acta Materialia, 61(13), 4887-4897.
[5] Senkov, O. N., Wilks, G. B., Miracle, D. B., Chuang, C. P., & Liaw, P. K. (2010). Refractory high-entropy alloys. Intermetallics, 18(9), 1758-1765.
[6] Senkov, O. N., Wilks, G. B., Scott, J. M., & Miracle, D. B. (2011). Mechanical properties of Nb25Mo25Ta25W25 and V20Nb20Mo20Ta20W20 refractory high entropy alloys. Intermetallics, 19(5), 698-706.
[7] Senkov, O. N., Miracle, D. B., Chaput, K. J., & Couzinie, J. P. (2018). Development and exploration of refractory high entropy alloys—A review. Journal of materials research, 33(19), 3092-3128.
[8] Senkov, O. N., Senkova, S. V., & Woodward, C. (2014). Effect of aluminum on the microstructure and properties of two refractory high-entropy alloys. Acta Materialia, 68, 214-228.
[9] Juan, C. C., Tsai, M. H., Tsai, C. W., Lin, C. M., Wang, W. R., Yang, C. C., ... & Yeh, J. W. (2015). Enhanced mechanical properties of HfMoTaTiZr and HfMoNbTaTiZr refractory high-entropy alloys. Intermetallics, 62, 76-83.
[10] Sheikh, S., Shafeie, S., Hu, Q., Ahlström, J., Persson, C., Veselý, J., ... & Guo, S. (2016). Alloy design for intrinsically ductile refractory high-entropy alloys. Journal of applied physics, 120(16), 164902.
[11] Wei, Y., Li, Y., Zhu, L., Liu, Y., Lei, X., Wang, G., ... & Gao, H. (2014). Evading the strength–ductility trade-off dilemma in steel through gradient hierarchical nanotwins. Nature communications, 5(1), 1-8.
[12] Verlinden, B., Driver, J., Samajdar, I., & Doherty, R. D. (2007). Thermo-mechanical processing of metallic materials. Elsevier.
[13] Hughes, D. A., & Hansen, N. (1997). High angle boundaries formed by

grain subdivision mechanisms. Acta materialia, 45(9), 3871-3886.
[14] Humphreys, F. J., & Hatherly, M. (2012). Recrystallization and related annealing phenomena. Elsevier.
[15] Holscher, M., Raabe, D., & Lucke, K. (1991). Rolling and recrystallization textures of bcc steels. Steel Research-Dusseldorf 62(12), 567-575.
[16] Li, Z., Pradeep, K. G., Deng, Y., Raabe, D., & Tasan, C. C. (2016). Metastable high-entropy dual-phase alloys overcome the strength–ductility trade-off. Nature, 534(7606), 227-230.
[17] Wei, Y., Li, Y., Zhu, L., Liu, Y., Lei, X., Wang, G., ... & Gao, H. (2014). Evading the strength–ductility trade-off dilemma in steel through gradient hierarchical nanotwins. Nature communications, 5(1), 1-8.
[18] Liu, L., Ding, Q., Zhong, Y., Zou, J., Wu, J., Chiu, Y. L., ... & Shen, Z. (2018). Dislocation network in additive manufactured steel breaks strength–ductility trade-off. Materials Today, 21(4), 354-361.
[19] Ming, K., Bi, X., & Wang, J. (2019). Strength and ductility of CrFeCoNiMo alloy with hierarchical microstructures. International Journal of Plasticity, 113, 255-268.